JOURNAL OF APPLIED ELECTROCHEMISTRY **26** (1996) 311–317

High performance copper oxide cathodes for high temperature solid-oxide fuel cells

C.-L. CHANG, T.-C. LEE, T.-J. HUANG*

Department of Chemical Engineering, National Tsing Hua University, Hsinchu, Taiwan 300, Republic of China

Received 27 March 1995; revised 4 July 1995

The cathodic polarization characteristics of CuO and $YBa_2Cu_3O_{7-\delta}$ electrodes were studied in the temperature range 600 to 800 °C and at oxygen partial pressures ranging from 10^{-4} to 0.21 atm. The activity of oxygen reduction on a CuO electrode is closely related to the electronic conductivity and the oxygen ion vacancy density in the surface layer of the electrode. The oxygen ion vacancies created in CuO by doping with Li and the modification of the electronic conductivity by adding Ag provide a new way of enhancing the activity of an oxide electrode for oxygen reduction. It is demonstrated that the rate limiting steps for oxygen reduction at high overpotential and low overpotential are oxygen adsorption and charge transfer on CuO, respectively.

List of symbols

F	Faraday constant
f	F/RT
i	current
i_0	exchange current
k^0	intrinsic rate constant of charge transfer
$N(\epsilon)$	electron density with an energy level ϵ
n	number of electrons
R	gas constant
T	temperature

Greek letters

α	transfer coefficient
σ	conductivity
η	overpotential
ϵ	energy level

1. Introduction

Solid oxide fuel cells possess several advantages over other types of fuel cell systems. The use of a solid electrolyte eliminates most corrosion and liquid management problems [1]. Moreover, the high operating temperature facilitates rapid electrode kinetics without the requirement for expensive noble metal electrocatalysts such as Pt for phosphoric acid fuel cells.

In earlier studies of the cathode, Tedmon *et al.* investigated various characteristic materials, such as Pt (metal), YSZ with a current collector grid (oxygen ion conductor), and Sr-doped $LaCoO_3$ (electronically conducting oxide) [2]. The Sr-doped Perovskite oxides such as $LaSrMO_3$(M = Co,Fe,Mn) have recently attracted much attention because these oxides can conduct both oxygen ions and electrons [1, 3–5]. However, these complex oxides have a more difficult preparation process, and their cathode performance is sensitive to their structural properties, including the stoichiometric ratio of elements and the oxygen content in the lattice.

Moreover, the mechanism of oxygen reduction on oxide electrodes remains unclear. In a previous study [6], a mathematical model was established to explore the oxygen reduction pathway on a $YBa_2Cu_3O_{7-\delta}$ electrode. However, preparing and designing a high performance oxide cathode for solid oxide fuel cells requires further information about the influence of the electronic conductivity and the oxygen ion vacancy density on the oxygen reduction activity. Therefore, in this work, a simple binary transition oxide, CuO, is considered as the cathode material.

A comparison of cathodic behaviour between CuO and $YBa_2Cu_3O_{7-\delta}$ revealed the importance of electronic conductivity and oxygen ion vacancy density of an oxide electrode for oxygen reduction activity. Several new approaches were devised for preparation of an oxide cathode material. Moreover, the cathode performance of CuO was tested and improved by modifying the oxygen ion vacancy density and the electronic conductivity.

2. Experimental details

2.1. *Materials*

$YBa_2Cu_3O_{7-\delta}$ (YBCO) powder with $0 < \delta < 0.7$, as purchased from Seattle Specialty Ceramics, USA, was mixed with glycerol for use as a cathode material.

Two methods were used to investigate the effect of oxygen ion vacancy density on the oxygen reduction activity of a CuO cathode. One was the addition of

* To whom correspondence should be addressed.

0021-891X

a less positive ion into the CuO lattice by doping with Li_2O. This method can produce oxygen ion vacancies in the CuO lattice [7, 8]. Using Kröger–Vink notation, the mechanism is [8]

$$Li_2O \Leftrightarrow 2Li'_{Cu} + Vö + Oo^x \quad (1)$$

and

$$[Vö] = \tfrac{1}{2}[Li'_{Cu}] \quad (2)$$

Hence, the substitution of two Li atoms for a Cu atom creates one Vö. Distinguishing the oxygen ion vacancy produced by the above method from that produced by the other method is necessary. Therefore, the oxygen ion vacancy produced by doping with Li_2O is defined as a type-I oxygen ion vacancy. The other method involves mixing CuO powder with yttria-stabilized zirconia (YSZ) powder, that is, a solid electrolyte having oxygen-ion conductivity, thereby producing oxygen ion vacancies among the interstices of the CuO particles. This kind of oxygen ion vacancy is defined as a type-II oxygen ion vacancy. The method of calculating the oxygen ion vacancy number has been described elsewhere [9, 10].

Type-I oxygen ion vacancies in the CuO lattice were created by impregnating the CuO powder with an aqueous solution of $LiNO_3$ with 5 and 10 mol % Li, respectively, for 24 h, and then drying for 24 h at 100 °C. The product was ground and pressed into a pellet. The pellet was calcined at 900 °C for 8 h in air. The lattice structure of the Li-doped CuO material was then characterized by X-ray powder diffraction using CuK_α radiation (Shimadzu XD-5). Type-II oxygen ion vacancies among the interstices of CuO particles were created by mixing the CuO powder with 10 and 35 mol % YSZ powder, respectively. The oxygen ion vacancy densities of various electrode materials produced by the above two methods are listed in Table 1. These materials were separately mixed with glycerol into pastes to serve as cathode materials.

The following methods were employed to examine the influence of the CuO electronic conductivity on oxygen reduction. The CuO powder was impregnated with an aqueous solution of $AgNO_3$ with 15 mol % Ag for 24 h, and then dried for 24 h at 100 °C. These CuO materials were separately mixed with glycerol into pastes to be employed as cathode materials. An Ag/CuO electrode was prepared by depositing an Ag film over the CuO electrode. A NiO/CuO electrode was also prepared by the same method.

For the solid electrolyte, a tube of 8 mol % yttria stabilized zirconia was used (Zircoa, USA), having a length of 145 mm, an inner diameter of 25.4 mm and a thickness of 3 mm.

Table 1. Oxygen ion vacancy of CuO electrodes

Cathode	*Vö/mol %*
5 mol % Li–CuO	2.5
10 mol % Li–CuO	5
10 mol % YSZ–CuO	0.85
35 mol % YSZ–CuO	2.5

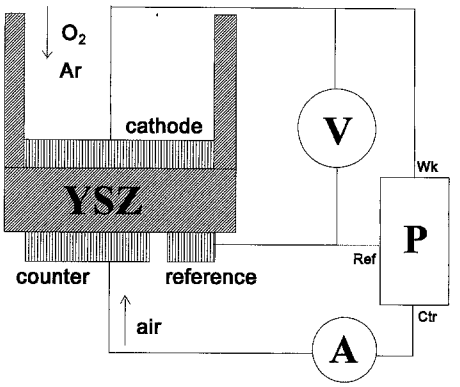

Fig. 1. Experimental apparatus.

2.2. *Electrode preparation*

The cathode material was painted on the inner bottom surface of the YSZ tube, and then calcined at 850 °C for 90 min. Platinum paste (Heraeus, USA) was painted on the outer bottom surface of the YSZ tube as the anode and the reference electrode, and then calcined at 850 °C for 90 min.

2.3. *Electrochemical measurement*

The polarization experiments were carried out using a three-electrode cell as shown in Fig. 1. The potentiostat (Pine RDE4) was used to control the cathode potential relative to the Pt reference electrode. The potential and current were measured by a digital multimeter (HP34401A) with a high input resistance (10 GΩ). To obtain a reproducible value, each data point of the cathode overpotential vs. current curve, required 20 min to reach steady state. The oxygen partial pressure ranged between 10^{-4} and 0.21 atm and the temperature between 600 and 800 °C.

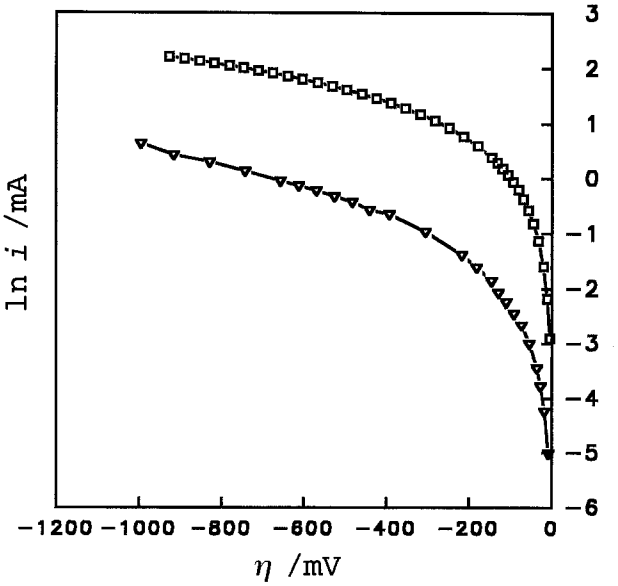

Fig. 2. Current–overpotential curves at 700 °C and $P_{O_2} = 10^{-2}$ atm. (□) YBCO electrode; (▽) CuO electrode.

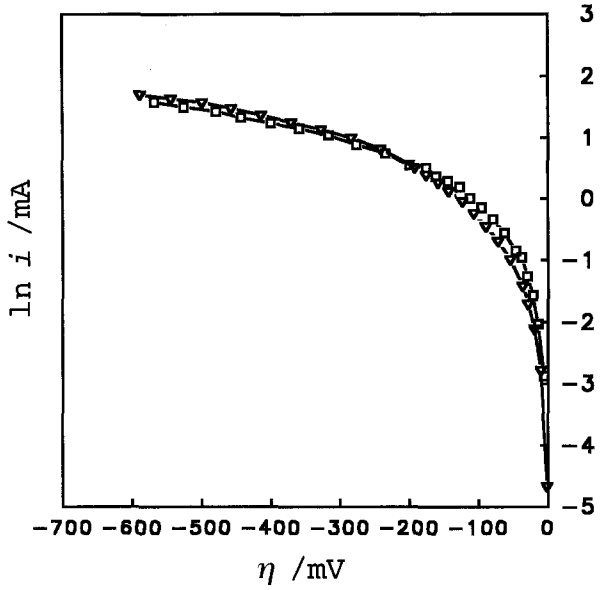

Fig. 3. Current–overpotential curves at 800 °C and $P_{O_2} = 10^{-2}$ atm. (□) YBCO electrode; (▽) CuO electrode.

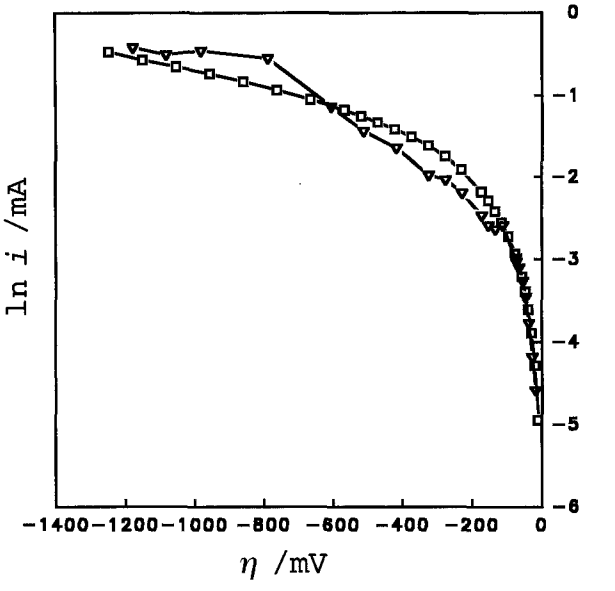

Fig. 5. Current–overpotential curves at 700 °C and $P_{O_2} = 10^{-4}$ atm. (□) YBCO electrode; (▽) CuO electrode.

3. Results and discussion

3.1. *Current–overpotential characteristics*

Figures 2 to 6 show the cathode current-overpotential behaviour of CuO and $YBa_2Cu_3O_{7-\delta}$ electrodes in the temperature range 600 to 800 °C and the oxygen partial pressure range 10^{-4} to 10^{-2} atm. At an oxygen partial pressure of 10^{-2} atm, as the temperature increases from 700 to 800 °C, the oxygen reduction activity of CuO is enhanced and comparable to that of $YBa_2Cu_3O_{7-\delta}$, as shown in Figs 2 and 3. Moreover, as shown in Figs 4 to 6, at a lower oxygen partial pressure of 10^{-4} atm, the oxygen reduction activity of CuO is enhanced as the temperature increases from 600 to 800 °C and becomes much better than that of $YBa_2Cu_3O_{7-\delta}$.

The electronic conductivity of a semiconductor is directly proportional to temperature. Hence, n-type CuO conductivity is enhanced by increase in temperature. On the other hand, the relation between the electronic conductivity and temperature for $YBa_2Cu_3O_{7-\delta}$ is more complex because the $YBa_2Cu_3O_{7-\delta}$ structure changes with temperature and oxygen partial pressure [11]. The oxygen content in the $YBa_2Cu_3O_{7-\delta}$ lattice decreases with increase in temperature at constant oxygen partial pressure [12]. The change of oxygen content in the $YBa_2Cu_3O_{7-\delta}$ lattice directly influences the electronic structure. It was demonstrated that the reduction of the oxygen content decreases the metallicity and finally, for a large δ (> 0.6), the $YBa_2Cu_3O_{7-\delta}$ transforms from a metal into a semiconductor state [11, 13].

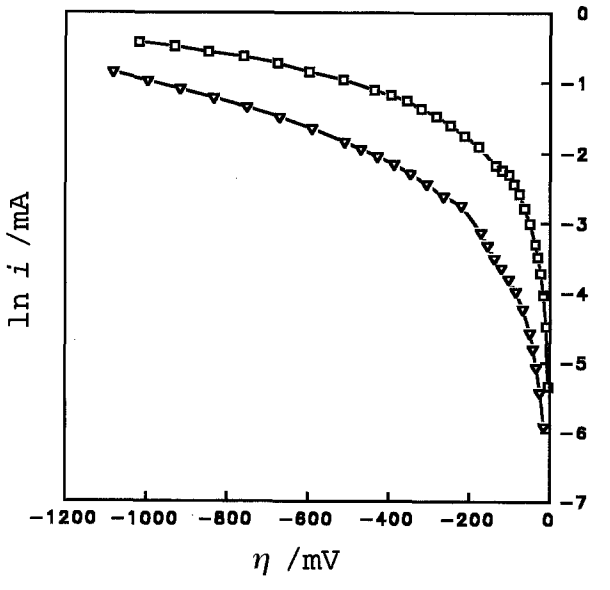

Fig. 4. Current–overpotential curves at 600 °C and $P_{O_2} = 10^{-4}$ atm. (□) YBCO electrode; (▽) CuO electrode.

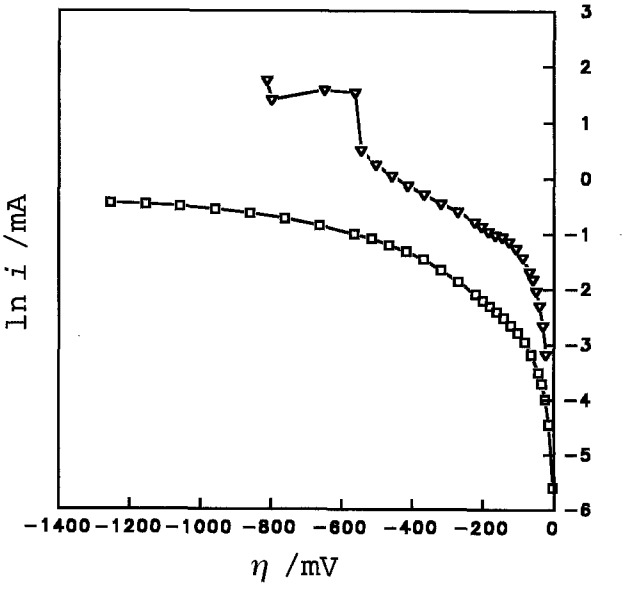

Fig. 6. Current–overpotential curves at 800 °C and $P_{O_2} = 10^{-4}$ atm. (□) YBCO electrode; (▽) CuO electrode.

The charge transfer reaction in the oxygen reduction process is given by

$$\tfrac{1}{2}O_2 + 2e^- + V\ddot{o} \xrightarrow{k^0} Oo^x \qquad (3)$$

According to quantum theory [14], it was demonstrated that

$$i_0 \propto k^0 \propto \sum N(\epsilon) W(\epsilon) e^{-\Delta G/RT} \qquad (4)$$

This equation reveals that the intrinsic rate of charge transfer is proportional to the electron density $N(\epsilon)$ with an energy level ϵ. As the temperature increases, the conductivity of CuO increases and that of $YBa_2Cu_3O_{7-\delta}$ decreases because of the transformation from a metal to a semiconductor state. Owing to this difference between the electronic properties of CuO and $YBa_2Cu_3O_{7-\delta}$, the CuO oxygen reduction activity at constant oxygen pressure is enhanced with increase in temperature and, subsequently, becomes better than that of $YBa_2Cu_3O_{7-\delta}$.

The above results illustrate that the charge transfer activity in the oxygen reduction process is closely related to the electronic conductivity of the oxide electrode. In contrast, previous studies show that the oxygen reduction activity of the metal electrodes, such as Pt, is not sensitive to the variation of the electronic conductivity with temperature because the rate limiting step is oxygen diffusion [15].

In addition, a dramatic change in the I/η behaviour occurs at an overpotential of around -600 mV, as shown in Fig. 6. It is probable that a reduction reaction occurs on CuO at low oxygen partial pressure of 10^{-4} atm, for example,

$$CuO + xe^- \longrightarrow CuO_{1-x} + xO^{2-} \qquad (5)$$

The CuO_{1-x} state may produce two effects: (a) CuO changes from being an intrinsic to an extrinsic semiconductor [16], thereby resulting in the enhancement in the electronic conductivity of CuO, and (b) the reduction process produces some oxygen ion vacancies on the CuO surface, thus influencing the activities for both oxygen adsorption and charge transfer [15, 16].

It may thus be concluded that electronic conductivity and oxygen ion vacancy are two important factors influencing the oxygen reduction activity of CuO. Further investigations were performed separately on the influence of the electronic conductivity and the oxygen ion vacancy density for oxygen reduction on CuO.

3.2. *Electronic conductivity*

The influence of the electronic conductivity of CuO electrodes on oxygen reduction is shown in Fig. 7. The exchange current is proportional to k^0 in Equation 4, which represents the intrinsic rate of an electrochemical reaction. The method suggested by Allen and Hickling [17] is used here to calculate the exchange current. The equation is

$$\eta = \frac{1}{\alpha nf} \ln[(1 - e^{nf\eta})/i] + \ln(i_0)/\alpha nf \qquad (6)$$

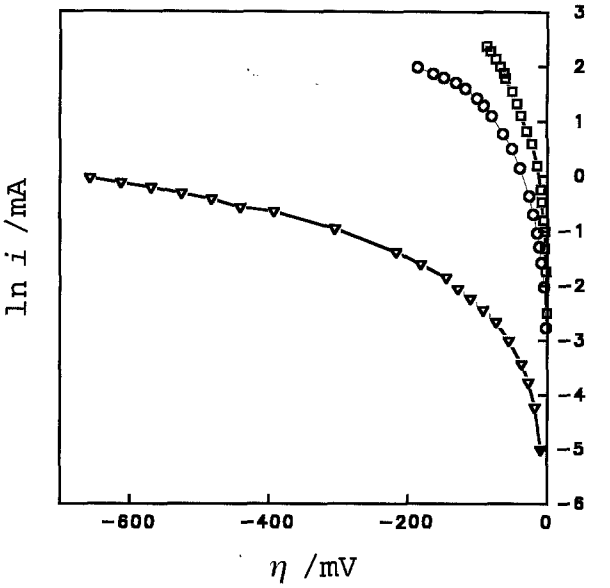

Fig. 7. Current–overpotential curves at 700 °C and $P_{O_2} = 10^{-2}$ atm. (□) Ag/CuO electrode; (○) 15 mol % Ag–CuO electrode; (▽) CuO electrode.

A plot of η against $\ln[(1 - e^{nf\eta})/i]$ yields an intercept of $\ln(i_0)/\alpha nf$ and a slope of $1/\alpha nf$.

As shown in Fig. 7, the exchange current of a CuO electrode increased from 0.0304 to 3.26 mA on a Ag/CuO electrode when an Ag film was deposited on the surface of a CuO electrode. The charge transfer reaction is proposed as

$$O_{(Ag/CuO)} + 2e^- + V\ddot{o}_{(CuO)} \longrightarrow Oo^x \qquad (7)$$

This equation shows that an Ag film with a high electronic conductivity can significantly enhance the charge transfer rate of a CuO electrode. In addition, comparison of the Ag/CuO electrode with the 15 mol % Ag–CuO electrode in Fig. 7, reveals that the electrode activity with a bulk doping of 15 mol % Ag in CuO is less than that with surface deposition of Ag on CuO for oxygen reduction. Moreover, the exchange current of the Ag/CuO electrode ($i_0 = 3.26$ mA) is larger than that of the 15 mol % Ag–CuO electrode ($i_0 = 1.0$ mA). In addition, it is noteworthy that the Ag amount in a Ag/CuO electrode is only 0.2 times that in a 15 mol % Ag–CuO electrode. The difference in the oxygen reduction activities of the above two electrodes shows that the electronic conductivity of the CuO surface layer is more significant than that of the bulk CuO. Ag dispersal in the surface layer of a CuO electrode by surface techniques is a preferable method than a Ag film deposited on a CuO electrode to decrease the volatilization losses of Ag.

The electronic conductivity of the CuO electrode should be modified so that the charge transfer step takes place predominantly on the CuO surface layer, not in the bulk CuO or at the CuO/YSZ interface. This will reveal how a good CuO cathode can be prepared by modifying the electronic conductivity. An optimal schematic design of a CuO cathode is shown in Fig. 8. While the surface layer of the CuO electrode should catalyze oxygen adsorption and

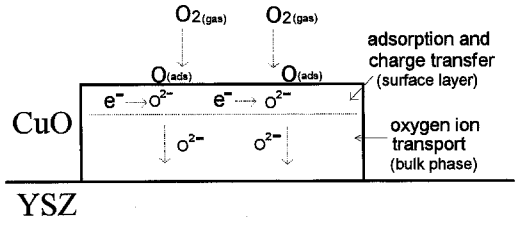

Fig. 8. An optimal schematic design of a CuO cathode.

charge transfer, the bulk CuO phase should act primarily as a medium for transferring oxygen anions. In a previous study of ceramic oxide $YBa_2Cu_3O_{7-\delta}$ electrodes [6], an oxygen reduction mechanism similar to that in Fig. 8 was proposed. Nevertheless, to our knowledge, the roles of surface layer and bulk phase in an oxide cathode are clarified here for the first time.

The above results show that the rate limiting step in oxygen reduction process on CuO is charge transfer at low overpotential because the exchange current is markedly enhanced by increasing the electronic conductivity of CuO. In addition, the I-η curves are consistent with the Butler–Volmer equation. On the other hand, as shown in Fig. 6, at low oxygen partial pressure (10^{-4} atm), the limiting current resulting from oxygen diffusion does not appear. This indicates that the diffusion step is not the rate limiting step in oxygen reduction process on CuO at high overpotential. In fact, the Ag film deposited on the CuO surface not only influences the electronic conductivity on the Ag/CuO interface but also increases the oxygen adsorption capability, since Ag is well known to be a strong adsorption catalyst for oxygen [16].

A p-type semiconductor, NiO, was deposited on the CuO surface. NiO and CuO are both semiconductors. However, the oxygen adsorption capability of p-type semiconductors is better than that of n-type semiconductors [16, 18]. As indicated in Fig. 9, the NiO film deposited over the CuO electrode clearly decreases the cathodic polarization at high overpotential.

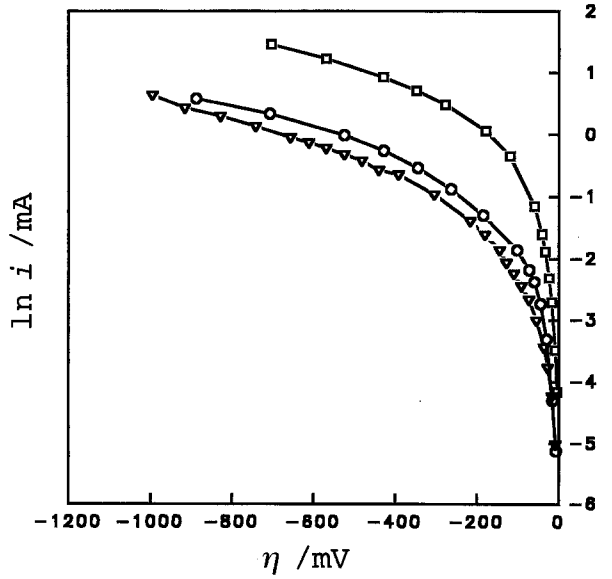

Fig. 9. Current–overpotential curves at 700 °C and $P_{O_2} = 10^{-2}$ atm. (□) NiO/CuO electrode; (▽) CuO electrode; (○) 35 mol % NiO–CuO electrode.

Therefore, at high overpotential, the rate limiting step of oxygen reduction on a CuO electrode is probably oxygen adsorption on the surface. However, CuO with a bulk doping of 35 mol % NiO does not significantly improve the polarization of a CuO electrode; in addition, its oxygen reduction activity is markedly less than that of the NiO/CuO electrode. This observation emphasizes the importance of the surface property on CuO, as shown in Fig. 8.

The above results demonstrate that the surface-layer property of a CuO electrode is the most influential factor responsible for CuO being a good cathode material for SOFCs. Furthermore, the charge transfer step and the oxygen adsorption step are the rate-limiting steps at low overpotential and high overpotential, respectively.

3.3. *Oxygen ion vacancy density*

In addition to the electronic conductivity, the oxygen ion vacancy must also be considered as a factor influencing the oxygen reduction activity of an oxide electrode. The influence of the oxygen ion vacancies in CuO on oxygen reduction was investigated separately from both the type-I vacancy and the type-II vacancy perspectives. The Li-doped CuO material represents CuO with the type-I oxygen ion vacancies in the lattice. In contrast, the YSZ–CuO material represents CuO with type-II oxygen ion vacancies among the interstices of CuO particles. The Li-doped CuO material lattice structure was characterized by X-ray powder diffraction. The patterns are shown in Fig. 10. Comparison of the diffraction lines of pattern (a) with those of pattern (b) indicates that the former, with the pretreatment of pressing into pellets and calcining at 900 °C, have a parallel shift. If the lattice expands or contracts uniformly, the diffraction lines merely shift position but do not increase in number [19]. Therefore, this figure indicates that, in the CuO lattice, the Li atom is substituted for the Cu site, thereby creating oxygen ion vacancies in the CuO lattice.

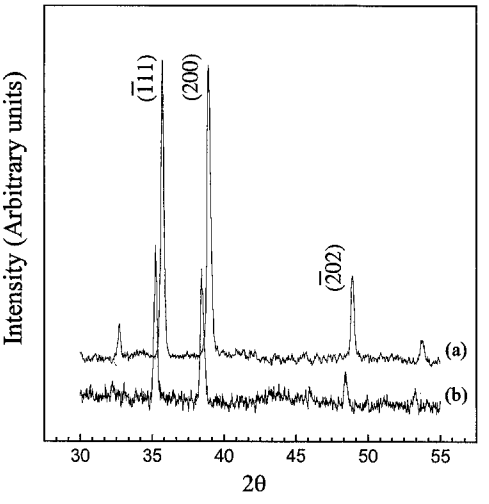

Fig. 10. X-ray diffraction patterns, (a) CuO doped by 5 mol % Li with the pretreatment of pressing into pellets and calcining at 900 °C for 9 h; (b) CuO doped by 5 mol % Li without the pretreatment of (a).

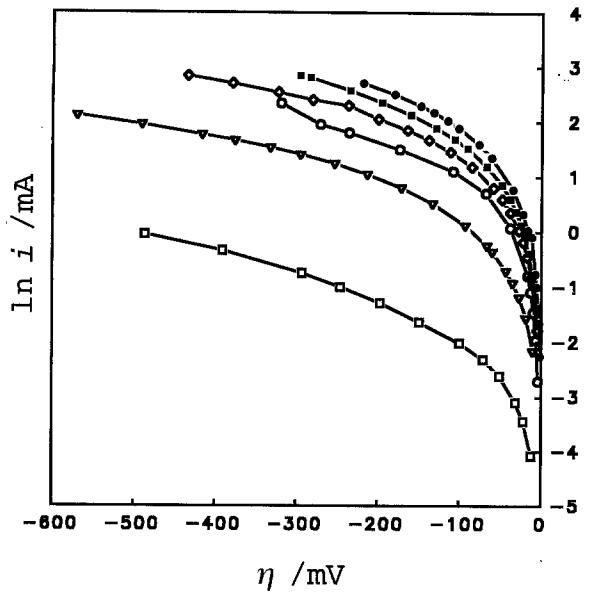

Fig. 11. Current–overpotential curves at 800 °C and P_{O_2} = 0.21 atm. (●) 5 mol % Li–CuO; (○) 10 mol % Li–CuO; (■) 10 mol % YSZ–CuO; (□) 35 mol % YSZ–CuO; (◇) YBCO; (▽) CuO.

The influence of the type-I and type-II oxygen ion vacancies on oxygen reduction on a CuO electrode is shown in Fig. 11. Notably, although the oxygen ion vacancy density of the modified CuO electrodes such as 5 mol % Li–CuO and 10 mol % YSZ–CuO is only slightly higher than that of the CuO electrode, their I/η characteristics are much better than that of the CuO electrode. Moreover, calculations by Equation 6 indicate that the exchange current of the 5 mol % Li–CuO electrode ($i_0 = 2.9$ mA) is much larger than that of the CuO electrode ($i_0 = 0.5$ mA). This difference shows that oxygen ion vacancies are beneficial to the charge transfer as shown in Equation 3. However, excessive oxygen ion vacancies are observed not to be beneficial to oxygen reduction on a CuO electrode. As shown in Fig. 11, the activity of the 10 mol % Li–CuO electrode with 5 mol % Vö (see Table 1) is less than that of the 5 mol % Li–CuO electrode with 2.5 mol % Vö. This is a result of the competition between the oxygen ion vacancy density and the electron density in CuO. Since the total conductivity consisting of the contributions from both ionic and electronic defects is

$$\sigma_{\text{total}} = \sigma_{\text{ion}} + \sigma_{\text{electron}} + \sigma_{\text{hole}} \quad (8)$$

an increase of the oxygen ion vacancy density must decrease the electron density in CuO [9, 10]. On the other hand, comparison of the cathodic polarization between 5 mol % Li–CuO and 35 mol % YSZ–CuO electrodes, which have the same oxygen vacancy density as shown in Table 1, reveals that the activity of 35 mol % YSZ–CuO for oxygen reduction is not only worse than that of 5 mol % Li–CuO, but also markedly less than that of the CuO electrode. This is because the electronic conductivity of CuO is lowered by the addition of YSZ, which is an electronic insulator. In addition, although a CuO electrode is intrinsically worse than a $YBa_2Cu_3O_{7-\delta}$ electrode for oxygen reduction, the CuO electrode modified by a minute number of oxygen ion vacancies, such as 5 mol % Li–CuO, shows superior activity to the $YBa_2Cu_3O_{7-\delta}$ electrode, as shown in Fig. 11.

These results illustrate that the oxygen ion vacancy can enhance the CuO electrode activity and an optimal ratio of the oxygen ion vacancy density to the electron density in CuO is necessary to produce a good CuO electrode for oxygen reduction. On the other hand, the oxygen ion vacancies created on a CuO surface have been found to be beneficial to oxygen adsorption [16, 18]. Hence, the optimal addition of oxygen ion vacancies in the CuO lattice should not only improve the activity of charge transfer, but also enhance the oxygen adsorption capability. In addition, these investigations of the oxygen ion vacancy and the electronic conductivity illustrate that the dramatic change of the I/η curve at high overpotential, as shown in Fig. 6, results from the influence of the oxygen ion vacancies created on the CuO surface.

The present results also demonstrate that, besides the factor of the electronic conductivity, the oxygen ion vacancy plays an influential role in the oxygen reduction activity over a CuO electrode. Therefore, it can be concluded that fabricating a high performance copper oxide cathode requires simultaneously considering the electronic conductivity and the oxygen ion vacancy density.

4. Conclusion

Charge transfer and oxygen adsorption are the rate limiting steps for oxygen reduction on CuO at low overpotential and high overpotential, respectively. It can be concluded that the surface layer properties on a CuO electrode plays a dominant role in the oxygen adsorption and charge transfer process. The CuO electrode activity for oxygen reduction is closely related to the electronic conductivity and the oxygen ion vacancy density on the surface, but not in the bulk of the CuO. The new approaches of creating oxygen vacancies by doping with Li and modifying the electronic conductivity by the addition of Ag can therefore be employed to fabricate high performance copper oxide cathodes for high temperature solid-state fuel cells.

Acknowledgement

The authors wish to thank the National Science Council of the Republic of China for financial support of this manuscript under contract NSC-81-0402-E-007-09.

References

[1] B. C. H. Steele, *J. Power Sources* **49** (1994) 1.
[2] C. S. Tedmon, H. S. Spacil and S. P. Mitoff, *J. Electrochem. Soc.* **116** (1969) 1170.
[3] Y. Takeda, R. Kanno, M. Noda, Y. Tomidda and O. Yamamoto, *ibid.* **134** (1987) 2656.

[4] J. V. Herle, A. J. McEvoy and K. R. Thampi, *Electrochim. Acta* **39** (1994) 1675.
[5] B. Gharbage, T. Pagnier and A. Hammou, *J. Electrochem. Soc.* **141** (1994) 211.
[6] C. L. Chang, T. C. Lee and T. J. Huang, *ibid.*, submitted.
[7] A. Clark, 'The Chemisorptive Bond', Academic Press, New York (1974) p. 80.
[8] N. Birks and G. H. Meier, 'Introduction to High Temperature Oxidation of Metals', Edward Arnold, London (1983) p. 191.
[9] P. J. Gellings and H. J. M. Bouwmeester, *Catalysis Today* **12** (1992) 1.
[10] E. C. Subbarao, 'Solid Electrolytes and Their Applications', Plenum Press, New York (1980).
[11] C. N. R. Rao, 'Chemistry of High Temperature Superconductors', World Scientific, New Jersey (1991) p. 126.
[12] K. Kishio, J. Shimoyama, T. Hasegawa, K. Kitazawa and K. Fueki, *Jpn. J. Appl. Phys.* **26** (1987) L1228.
[13] W. E. Pickett, R. E. Cohen and H. Krakauer, *Phys. Rev.* **B42** (1990) 88764.
[14] J. O'M. Bockris and B. E. Conway, 'Modern Aspects of Electrochemistry', Plenum Press, New York (1972) p. 5.
[15] K. Kinoshita, 'Electrochemical Oxygen Technology', John Wiley & Sons, New York (1992) p. 72.
[16] G. C. Bond, 'Heterogeneous Catalysis', Clarendon, Oxford (1987) p. 45.
[17] P. A. Allen and A. Hickling, *Trans. Faraday Soc.* **53** (1957) 1626.
[18] W. E. Garner, 'Chemistry of The Solid State', Butterworths, London (1955) p. 398.
[19] B. D. Cullity, 'Elements of X-ray Diffraction', Addison-Wesley, New York (1978) p. 340.